Nat. Hazards Earth Syst. Sci., 18, 241–256, 2018
https://doi.org/10.5194/nhess-18-241-2018

Natural Hazards and Earth System Sciences
Open Access
EGU

Width of surface rupture zone for thrust earthquakes: implications for earthquake fault zoning

Paolo Boncio[1], **Francesca Liberi**[1], **Martina Caldarella**[1], **and Fiia-Charlotta Nurminen**[2]

[1]CRUST, DiSPuTer, "G. D'Annunzio" University of Chieti-Pescara, Chieti, 66100, Italy
[2]Oulu Mining School, University of Oulu, Oulu, 90014, Finland

Correspondence: Paolo Boncio (paolo.boncio@unich.it)

Received: 8 April 2017 – Discussion started: 19 April 2017
Revised: 21 October 2017 – Accepted: 14 November 2017 – Published: 19 January 2018

Abstract. The criteria for zoning the surface fault rupture hazard (SFRH) along thrust faults are defined by analysing the characteristics of the areas of coseismic surface faulting in thrust earthquakes. Normal and strike–slip faults have been deeply studied by other authors concerning the SFRH, while thrust faults have not been studied with comparable attention.

Surface faulting data were compiled for 11 well-studied historic thrust earthquakes occurred globally ($5.4 \leq M \leq 7.9$). Several different types of coseismic fault scarps characterize the analysed earthquakes, depending on the topography, fault geometry and near-surface materials (simple and hanging wall collapse scarps, pressure ridges, fold scarps and thrust or pressure ridges with bending-moment or flexural-slip fault ruptures due to large-scale folding). For all the earthquakes, the distance of distributed ruptures from the principal fault rupture (r) and the width of the rupture zone (WRZ) were compiled directly from the literature or measured systematically in GIS-georeferenced published maps.

Overall, surface ruptures can occur up to large distances from the main fault (~ 2150 m on the footwall and ~ 3100 m on the hanging wall). Most of the ruptures occur on the hanging wall, preferentially in the vicinity of the principal fault trace ($> \sim 50$ % at distances $< \sim 250$ m). The widest WRZ are recorded where sympathetic slip (Sy) on distant faults occurs, and/or where bending-moment (B-M) or flexural-slip (F-S) fault ruptures, associated with large-scale folds (hundreds of metres to kilometres in wavelength), are present.

A positive relation between the earthquake magnitude and the total WRZ is evident, while a clear correlation between the vertical displacement on the principal fault and the total WRZ is not found.

The distribution of surface ruptures is fitted with probability density functions, in order to define a criterion to remove outliers (e.g. 90 % probability of the cumulative distribution function) and define the zone where the likelihood of having surface ruptures is the highest. This might help in sizing the zones of SFRH during seismic microzonation (SM) mapping.

In order to shape zones of SFRH, a very detailed earthquake geologic study of the fault is necessary (the highest level of SM, i.e. Level 3 SM according to Italian guidelines). In the absence of such a very detailed study (basic SM, i.e. Level 1 SM of Italian guidelines) a width of ~ 840 m (90 % probability from "simple thrust" database of distributed ruptures, excluding B-M, F-S and Sy fault ruptures) is suggested to be sufficiently precautionary. For more detailed SM, where the fault is carefully mapped, one must consider that the highest SFRH is concentrated in a narrow zone, ~ 60 m in width, that should be considered as a fault avoidance zone (more than one-third of the distributed ruptures are expected to occur within this zone).

The fault rupture hazard zones should be asymmetric compared to the trace of the principal fault. The average footwall to hanging wall ratio (FW : HW) is close to 1 : 2 in all analysed cases.

These criteria are applicable to "simple thrust" faults, without considering possible B-M or F-S fault ruptures due to large-scale folding, and without considering sympathetic slip on distant faults. Areas potentially susceptible to B-M or F-S fault ruptures should have their own zones of fault rupture hazard that can be defined by detailed knowledge of the structural setting of the area (shape, wavelength, tightness and lithology of the thrust-related large-scale folds) and by

geomorphic evidence of past secondary faulting. Distant active faults, potentially susceptible to sympathetic triggering, should be zoned as separate principal faults.

The entire database of distributed ruptures (including B-M, F-S and Sy fault ruptures) can be useful in poorly known areas, in order to assess the extent of the area within which potential sources of fault displacement hazard can be present.

The results from this study and the database made available in the Supplement can be used for improving the attenuation relationships for distributed faulting, with possible applications in probabilistic studies of fault displacement hazard.

1 Introduction

Coseismic surface ruptures during large earthquakes can produce damage to buildings and facilities located on or close to the trace of the active seismogenic fault. This is known as surface fault rupture hazard (SFRH), a localized hazard that could be avoided if a detailed knowledge of the fault characteristics is achieved. The mitigation of SFRH can be faced by strategies of fault zoning and avoidance or, alternatively, by (or together with) probabilistic estimates of fault displacement hazard (e.g. Youngs et al., 2003; Petersen et al., 2011). Both strategies need to employ, as accurately as possible, the location of the active fault trace, the expected displacement on the principal fault (PF; i.e. *principal faulting* in Youngs et al., 2003; see below for the definition), the deformation close to the PF, and the distribution of other faulting and fracturing away from it (i.e. *distributed faulting* in Youngs et al., 2003; see below for the definition). While the general geometry and the expected displacement of the PF can be obtained through a detailed geological study and the application of empirical relationships (e.g. Wells and Coppersmith, 1994), the occurrence of distributed faulting close to and away from the PF rupture is particularly difficult to predict, and only direct observations from well-documented case studies may provide insights on how distributed faulting is expected to occur (e.g. shape and size of rupture zones, attenuation relationships for distributed faulting).

A reference example of fault zoning strategy for mitigating SFRH is the Alquist–Priolo Earthquake Fault Zoning Act (A-P Act), adopted by the state of California (USA) in 1972 (e.g. Bryant and Hart, 2007). The A-P Act defines regulatory zones around active faults (earthquake fault zones, EFZs), within which detailed geologic investigations are required prior to building structures for human occupancy. The boundaries of the EFZs are placed 150–200 m away from the trace of major active faults, or 60–90 m away from well-defined minor faults, with exceptions where faults are complex or not vertical. Moreover, the A-P Act defines a minimum distance of 50 ft (15 m) from the well-defined fault trace within which structures designed for human occupancy cannot be built (fault setback), unless proven otherwise. Similarly, the New Zealand guidelines for development of land on or close to active faults (Kerr et al., 2003) define a fault avoidance zone to ensure life safety. Fault avoidance zones on district planning maps will allow a council to restrict development within the fault avoidance zone and take a risk-based approach to development in built-up areas. The risk-based approach combines the key elements of fault recurrence interval, fault complexity and building importance category. The guidelines recommend a minimum buffer of 20 m either sides of the known fault trace (or the likely rupture zone), unless detailed fault studies prove that the deformed zone is less than that.

Recently, in Italy the Department for Civil Protection published guidelines for land management in areas affected by active and capable faults. For the purpose of the guidelines, an active and capable fault is defined as a fault with demonstrated evidence of surface faulting during the last 40 000 years (Technical Commission for Seismic Microzonation, 2015; SM Working Group, 2015). The guidelines are a tool for zoning active and capable faults during seismic microzonation (SM). They also contain a number of recommendations to assist land managers and planners. The fault zones vary at different levels of SM. In the basic SM (Level 1 SM according to SM Working Group, 2015), the active fault is zoned with a wide warning zone that is conceptually equivalent to the EFZ of the A-P Act. The zone should include all the reasonable inferred fault rupture hazard of both the PF and other secondary faults, and should account for uncertainties in mapping the fault trace. The guidelines recommend a width of the warning zone to be 400 m. Within the warning zone, the most detailed level of SM (Level 3 SM) is recommended; this should be mandatory before new development. Level 3 SM implies a detailed earthquake geology study of the fault. After completing that study, a new, more accurate fault zoning is achieved. This includes a 30 m wide fault avoidance zone around the accurately defined fault trace. If some uncertainties persist after Level 3 studies, such as uncertainties about fault trace location or about the possibility of secondary faulting away from the PF, the guidelines suggest the use of a wider zone called susceptible zone, within which development is restricted. Uncertainties within the susceptible zone can be reduced by additional site-specific investigations. The guidelines recommend a width of the susceptible zone to be 160 m, but the final shape and size of the zone depend on the local geology and the level of accuracy reached during Level 3 SM studies. Both fault avoidance and susceptible zones can be asymmetric compared with the main fault trace, with recommended footwall to hanging wall ratios of 1 : 4, 1 : 2 and 1 : 1 for normal, thrust and strike–slip faults, respectively.

Shape and width of the zones in the Italian guidelines are based mostly on data from normal faulting earthquakes (e.g. Boncio et al., 2012). In general, the fault displacement hazard of normal and strike–slip faults (e.g. Youngs et al., 2003;

Petersen et al., 2011) has been much more studied than that of thrust faults. Zhou et al. (2010) analysed the width of the surface rupture zones of the 2008 Wenchuan earthquake focusing on the rupture zone close to the PF, with implications on the setback distance. However, to our knowledge, a global data compilation from well-documented surface thrust faulting earthquakes aimed at analysing the characteristics of the WRZ is lacking in the scientific literature.

The objectives of this work are (1) to compile data from well-studied surface faulting thrust earthquakes globally (we analysed 11 earthquakes with magnitudes ranging from 5.4 to 7.9), (2) to analyse statistically the distribution of surface ruptures compared to the PF and the associated WRZ, and (3) to compare the results with the Italian guidelines and discuss the implications for earthquake fault zoning.

2 Methodology

This work analyses the data from 11 well-studied historic surface faulting thrust earthquakes occurred worldwide during the last few decades (Table 1). These historic earthquakes range in magnitude (M_w) from 5.4 to 7.9 and belong to different tectonic settings, such as continental collision (Spitak, 1988; Kashmir, 2005; Wenchuan, 2008), fold-and-thrust belt (El Asnam, 1980), oceanic–continental or continental–continental collision in large-scale subduction systems (Chi-Chi, 1999; Nagano, 2014), transform plate boundary (San Fernando, 1971; Coalinga-Nunez, 1983) and intraplate regions (Marryat Creek, 1986; Tennant Creek, 1988; Killari, 1993).

We compiled data from the literature of both principal and distributed faulting. As defined by Youngs et al. (2003), principal faulting is displacement along the main fault responsible for the release of seismic energy during the earthquake. At the surface, the displacement may occur along a single narrow trace of the PF or within a metres-scale wide fault zone. Distributed faulting is displacement on other faults in the vicinity of the PF rupture. Distributed ruptures are often discontinuous and may occur tens of metres to kilometres away from the PF rupture. Displacement may occur on secondary faults connected with the PF, such as splay faults, or on pre-existing faults structurally unconnected with the main fault (called here sympathetic fault ruptures). In particular, for the purpose of this work, the following parameters were extracted from the literature listed in Table 1: (i) displacement (vertical, horizontal and net slip, if available) on the PF rupture and coordinates of the referred measurement points for strands of the PF having associated distributed ruptures (DRs), (ii) distance from the PF to the DRs (r in Fig. 1), distinguishing between the ones on hanging wall and on footwall, (iii) displacement on DRs (if available), (iv) width of the rupture zone (WRZ), distinguishing between the ones on hanging wall and on footwall, and (v) scarp type (Fig. 2).

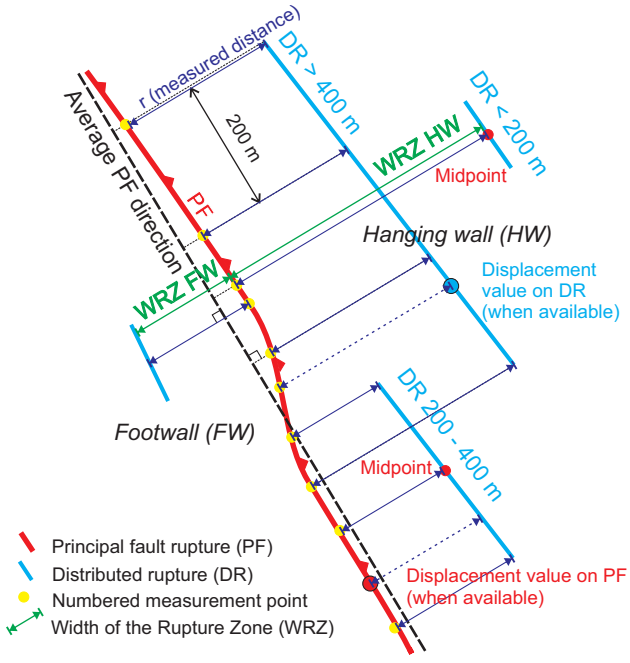

Figure 1. Sketch synthesizing the methodology used for measuring the "r" and WRZ data. Distance between the PF rupture and distributed rupture is measured along the line perpendicular to the auxiliary line indicating the average direction of the PF, always between the faults. Points with displacement values are prioritized at the expense of the 200 m metrics (the closest measurement point) when reasonable, in order to avoid over-measuring.

When available, the surface rupture data were compiled directly from published tables (e.g. Chi-Chi, 1999; Wenchuan, 2008), but in most of the other cases the rupture data were measured from the maps published by the previous authors that were GIS-georeferenced for the purpose of this work. Figure 1 displays the technique used for measuring the distance between the PF rupture and the DRs, which allowed us to sample the rupture zone systematically and in reasonable detail. The measurements carried out on the published maps are illustrated in Figs. S1 to S11 of the Supplement, and the entire compiled database is made available in Table S1 of the Supplement. The accuracy of the measurements depends on the scale of the original maps and on the level of detail reported in the maps (the original scale of the published maps is reported in the figures of the Supplement). In this work only detailed maps were considered, and uncertain or inferred ruptures were not taken into account. It is important to specify that the database made available in Table S1 can be used only for analysing distributed faulting. Data on the PF rupture are not complete, because the strands of the PF without DRs were not included in the database.

In order to distinguish the PF rupture, the following aspects were considered: (1) larger displacement compared to distributed faulting, (2) longer continuity, and (3) coincidence or nearly coincidence with major tec-

Table 1. Earthquakes used for analysing the width of the rupture zone (WRZ).

Earthquake	Date	Magnitude	Kin.[a]	SRL[b] (km)	MD[c] (m)	Depth (km)	References[d] for earthquake parameters (a) and WRZ calculation (b)
1) San Fernando, CA, USA	9 Feb 1971	$M_S = 6.5$, $M_W = 6.6$	R-LL	16	2.5	8.9 (USGS)	(a) 1 (b) 2
2) El Asnam, Algeria	10 Oct 1980	$M_S = 7.3$, $M_W = 7.1$	R	31	6.5	10 (USGS)	(a) 1 (b) 3, 4, 5
3) Coalinga (Nunez), CA, USA	11 Jun 1983	$M_S = 5.4$, $M_W = 5.4$	R	3.3	0.64	2.0 (USGS)	(a) 1 (b) 6
4) Marryat Creek, Australia	30 Mar 1986	$M_S = 5.8$, $M_W = 5.8$	R-LL	13	1.3	3.0	(a) 1, 7 (b) 8, 9
5) Tennant Creek, Australia	22 Jan 1988 (3 events)	$M_S = 6.3$, $M_W = 6.3$ $M_S = 6.4$, $M_W = 6.4$ $M_S = 6.7$, $M_W = 6.6$	R R-LL R	10.2 6.7 16	1.3 1.17 1.9	2.7 3.0 4.2	(a) 1, 10 (b) 11
6) Spitak, Armenia	7 Dec 1988	$M_S = 6.8$, $M_W = 6.8$	R-RL	25	2.0	5.0–7.0	(a) 1, 12 (b) 13
7) Killari, India	29 Sep 1993	$M_S = 6.4$, $M_W = 6.2$	R	5.5	0.5	2.6	(a) 14, 15 (b) 15, 16
8) Chi-Chi, Taiwan	20 Sep 1999	$M_W = 7.6$	R-LL	72	16.4	8.0	(a) 17, 18 (b) 19, 20, 21, 22, 23, 24, 25, 26, 27, 28, 29, 30, 31, 32, 33, 34, 35, 36, 37, 38, 39, 40, 41
9) Kashmir, Pakistan	8 Oct 2005	$M_W = 7.6$	R	70	7.05 (v)	< 15.0	(a) 42, 43 (b) 43, 44
10) Wenchuan, China	12 May 2008	$M_W = 7.9$	R-RL	240	6.5 (v) 4.9 (h)	19.0 (USGS)	(a) 45 (b) 46, 47, 48, 49, 50, 51, 52, 53, 54, 55, 56, 57, 58, 59
11) Nagano, Japan	22 Nov 2014	$M_W = 6.2$	R	9.3	1.5 (v)	4.5	(a) 60, 62 (b) 60, 61, 62

[a] Kin. (kinematics): R: reverse; LL: left lateral; RL: right lateral.
[b] SRL: surface rupture length.
[c] MD: maximum displacement (vector sum, unless otherwise specified; v: vertical; h: horizontal).
[d] References: 1: Wells and Coppersmith (1994), 2: US Geological Survey Staff (1971), 3: Yelding et al. (1981), 4: Philip and Meghraoui (1983), 5: Meghraoui et al. (1988), 6: Rymer et al. (1990), 7: Fredrich et al. (1988), 8: Bowman and Barlow (1991), 9: Machette et al. (1993), 10: McCaffrey (1989), 11: Crone et al. (1992), 12: Haessler et al. (1992), 13: Philip et al. (1992), 14: Lettis et al. (1997), 15: Seeber et al. (1996), 16: Rajendran et al. (1996), 17: Wesnousky (2008), 18: Shin and Teng (2001), 19: Kelson et al. (2001), 20: Kelson et al. (2003), 21: Angelier et al. (2003), 22: Bilham and Yu (2000), 23: Chang and Yang (2004), 24: Chen et al. (2000), 25: Chen et al. (2003), 26: Faccioli et al. (2008), 27: Huang et al. (2008), 28: Huang et al. (2000), 29: Huang (2006), 30: Kawashima (2002), 31: Konagai et al. (2006), 32: Lee and Loh (2000), 33: Lee et al. (2001), 34: Lee and Chan (2007), 35: Lee et al. (2003), 36: Lee et al. (2010), 37: Lin (2000), 38: Ota et al. (2001), 39: Ota et al. (2007a), 40: Ota et al. (2007b), 41: Central Geological Survey (MOEA at http://gis.moeacgs.gov.tw/gwh/gsb97-1/sys8/index.cfm), 42: Avouac et al. (2006), 43: Kaneda et al. (2008), 44: Kumahara and Nakata (2007), 45: Xu et al. (2009), 46: Liu-Zeng et al. (2009), 47: Liu-Zeng et al. (2012), 48: Yu et al. (2009), 49: Yu et al. (2010), 50: Zhou et al. (2010), 51: Zhang et al. (2013), 52: Chen et al. (2008), 53: Dong et al. (2008a), 54: Dong et al. (2008b), 55: Liu-Zeng et al. (2010), 56: Wang et al. (2010), 57: Xu et al. (2008), 58: Zhang et al. (2012), 59: Zhang et al. (2010), 60: Okada et al. (2015), 61: Ishimura et al. (2015), 62: Lin et al. (2015).

tonic/geomorphologic features, such as the trace of the main fault mapped before the earthquake on geologic maps.

The distance between the PF and the DRs was measured perpendicularly to the average direction of the PF, which was defined by visual inspection of the published maps, averaging the direction of first-order sections of the PF (few to several kilometres long). Particular attention was paid to variations of the average strike, in order to avoid duplicate measurements. In some places, the PF is discontinuous. In a few of those cases, and only for the purpose of measuring the distance of DRs from the main fault trace, we drew the trace of the main geologic fault between nearby discontinuous ruptures by using major tectonic/geomorphologic features from available maps (inferred trace of the principal geologic fault in Figs. S1, S2, S8–S11). In these cases the distance "r" was measured between the DR and this inferred principal geologic fault.

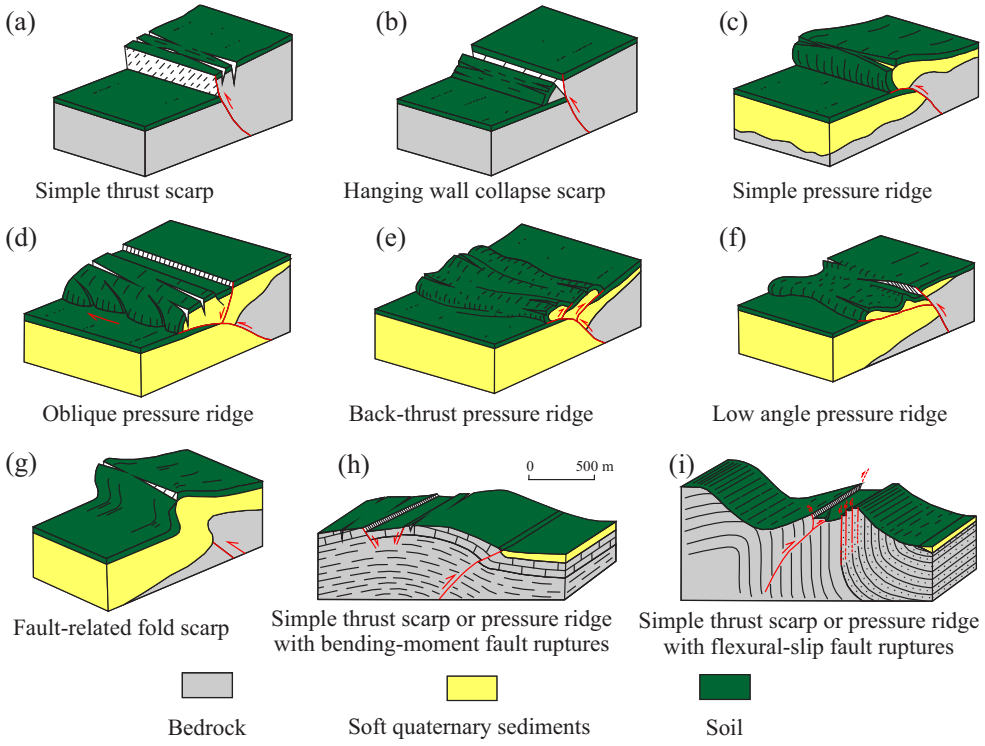

Figure 2. Scarp type classification (modified after Philip et al., 1992 and Yu et al., 2010). The scarp types **(h)** and **(i)** are associated with large-scale folds (hundreds of metres to kilometres in wavelength) and are from Philip and Meghraoui (1983).

DRs were measured every 200 m along-strike the PF. In order to prevent short ruptures being missed or under-sampled during measurement, ruptures shorter than 200 m were measured at the midpoint, and ruptures between 200 and 400 m long were measured at the midpoint and endpoints (Fig. 1). Moreover, all the points having displacement information on DRs were measured. All the points with displacement values on the PF rupture were also measured if DRs were associated with that strand of the PF. A particular metrics was used for the Sylmar segment of the San Fernando 1971 rupture zone (Fig. S1), where most of the distributed faulting was mapped along roads, resulting in a very discontinuous pattern of surface ruptures. In order to have a database of measurements statistically equivalent with respect to the other studied earthquakes, various measurement logics were used in order to sample ruptures at distances that equal more or less 200 m (see Fig. S1 for details).

All the DRs reported in the published maps as of primary (i.e. tectonic) origin were measured. Only the "Beni Rached" rupture zone of the 1981 El Asnam earthquake (Fig. S2) was not measured. It consists of normal fault ruptures interpreted to be related to either or both of the following (Yelding et al., 1981; Philip and Meghraoui, 1983): (1) very large gravitational sliding and (2) surface response of an unconstrained deep tectonic fault also responsible for the 1954 *M* 6.7 earthquake. Therefore, we avoided measuring the rupture due to the large uncertainties concerning its primary origin.

Some DRs reasonably unconnected with the main seismogenic fault were classified as sympathetic fault ruptures (Sy; Figs. S1, S2 and S5). We included in this category a rupture on a pre-existing thrust fault located more than 2 km in the hanging wall of the Chi-Chi 1999 PF rupture, due to its large distance from the main fault trace compared to all the other DRs (Tsauton East fault, Fig. S8), but a deep connection with the main seismogenic fault is possible (Ota et al., 2007a).

The measured ruptures have been classified according to the scarp types illustrated in Fig. 2 – alternatively the scarp type was classified as "unknown". Scarp types from "a" to "g" (Fig. 2) follow the scheme proposed by Philip et al. (1992), integrated with the classification of Yu et al. (2010). In the case of steeply dipping faults, a simple thrust scarp in bedrock (type a) or a hanging wall collapse scarp in bedrock or in brittle unconsolidated material (type b) are produced. In the case of low-angle faults and the presence of soft-sediment covers, various types of pressure ridges (types c–f) can be observed, depending on the displacement, sense of slip and behaviour of near-surface materials. In the presence of shallow blind faults, a fault-related fold scarp may be formed (type g). Moreover, in this study two additional structural contexts were distinguished, which are characterized by the occurrence of bending-moment and flexural-

slip fault ruptures (Yeats, 1986), associated with large-scale folds (hundreds of metres to kilometres in wavelength). Both of these occurred widely during the 1980 El Asnam earthquake (Philip and Meghraoui, 1983). Bending-moment faults (type h in Fig. 2) are normal faults that are formed close to the hinge zone of large-scale anticlines (extensional faults at the fold extrados in Philip and Meghraoui, 1983), while flexural-slip faults (type i) are faults that are formed due to differential slip along bedding planes on the limbs of a bedrock fold. Bending-moment DRs associated with small-scale folds (metres to dozens of metres in wavelength), which form at the leading edge of the thrust, belong to scarp types c–g.

3 Width of the rupture zone (WRZ): statistical analysis

The most impressive and recurrent measured features are ruptures occurring along pre-existing fault traces and on the hanging wall, as the result of the reactivation of the main thrust at depth. Distributed ruptures are mainly represented by synthetic and antithetic faults, which are parallel to or branching from the main fault. Fault segmentation and en échelon geometries are common in transfer zones or in oblique-slip earthquakes.

The collected data were analysed in order to evaluate the WRZ, measured perpendicularly to the PF rupture. Figure 3 shows frequency distribution histograms of the distance of distributed ruptures from the PF (r) for all the analysed earthquakes. On the x axis (distance), zero indicates the PF, whereas the negative values refer to the footwall and the positive values refer to the hanging wall. In particular, in Fig. 3a we distinguished the scarps with bending-moment (B-M), flexural-slip (F-S) or sympathetic (Sy) fault ruptures from the other types; in Fig. 3b the scarps without B-M, F-S or Sy fault ruptures are distinguished by scarp types, and in Fig. 3c the scarps with B-M, F-S or Sy fault ruptures are distinguished by earthquake. In general, although the values span over a large interval (−2150 m in the footwall; 3100 m in the hanging wall), most of them occur in the proximity of the PF and display an asymmetric distribution between hanging wall and footwall.

In Fig. 3b the DRs data (excluding scarps with B-M, F-S and Sy fault ruptures) are distinguished by scarp type. Simple pressure ridges with narrow WRZ prevail. Larger WRZ characterizes back-thrust, low-angle and oblique pressure ridges, implying that the main thrust geometry, the local kinematics and the near-surface rheology have a significant control in strain partitioning with consequences on the WRZ, as expected.

The occurrence of B-M or F-S fault ruptures is strictly related to the structural setting of the earthquake area. In particular, B-M fault ruptures, which are related to the presence of large-scale hanging wall anticlines, were clearly observed in the El Asnam 1980 (Philip and Meghraoui, 1983) and Kashmir 2005 (southern part of central segment; Kaneda et al., 2008; Sayab and Khan, 2010) earthquakes. A wide extensional zone (1.8 km long in the E–W direction; 1.3 km wide) formed on the eastern hanging wall side of the Sylmar segment of the San Fernando 1971 surface rupture. The interpretation of such an extensional zone is not straightforward. Nevertheless, the presence of a macro-anticline in the hanging wall of the Sylmar fault is indicated by subsurface data (Mission Hill anticline; Tsutsumi and Yeats, 1999). Though it is not possible to clearly classify these structures as B-M faults in the strict sense, it seems reasonable to interpret them as generic fold-related secondary extensional faults. Therefore, they were plotted in Fig. 3a and c together with B-M fault ruptures. F-S fault ruptures were observed on the upright limb of a footwall syncline in the El Asnam 1980 earthquake.

Rupturing close to the main fault ($r < 150$ m) is prevalently caused by processes that are similar for all the scarp types (Fig. 3b), but for larger distances the distributed faulting can be affected by other processes such as large-scale folding or sympathetic reactivation of pre-existing faults (Fig. 3a and c), contributing significantly in widening the WRZ.

For the analysis of the statistical distribution of "r", the collected data were fitted with a number of probability density functions by using the commercial software EasyFitProfessional©V.5.6 (http://www.mathwave.com), which finds the probability distribution that best fits the data and automatically tests the goodness of the fitting. We decided to analyse both the database without B-M, F-S and Sy fault ruptures (called here "simple thrust" DRs; Fig. 4) and the entire database of distributed ruptures without filtering (Fig. 5). The aim is to analyse separately (1) DRs that can be reasonably related only to (or preferentially to) the coseismic propagation to the ground surface of the main fault rupture (they are expected to occur in a rather systematic way compared to the main fault trace) and (2) DRs that are affected also by other, non-systematic structural features, mostly related to large-scale coseismic folding. The hanging wall and footwall data were fitted separately and the results are synthesized in Figs. 4 and 5, where the best fitting probability density curves and the cumulative distribution curves are shown.

For "simple thrust" DRs, the hanging wall data (Fig. 4a and b) has a modal value of 7.1 m. The 90 % probability (0.9 of the cumulative distribution function, HW90) seems to be a reasonable value to cut off the outliers (flat part of the curves). It corresponds to a distance of ~ 575 m from the PF. From a visual inspection of the histogram (Fig. 4b), there is an evident sharp drop of the data approximately at the 35 % probability (HW35), corresponding to a distance of ~ 40 m from the PF. The second sharp drop of the data in the histogram occurs close to the 50 % probability (HW50, corresponding to ~ 80 m from the PF). Also the third quartile is shown (HW75), corresponding to a distance of ~ 260 m from the main fault. The widths of the zones for the different probabilities (90, 75, 50 and 35 %) are listed in Table 2a.

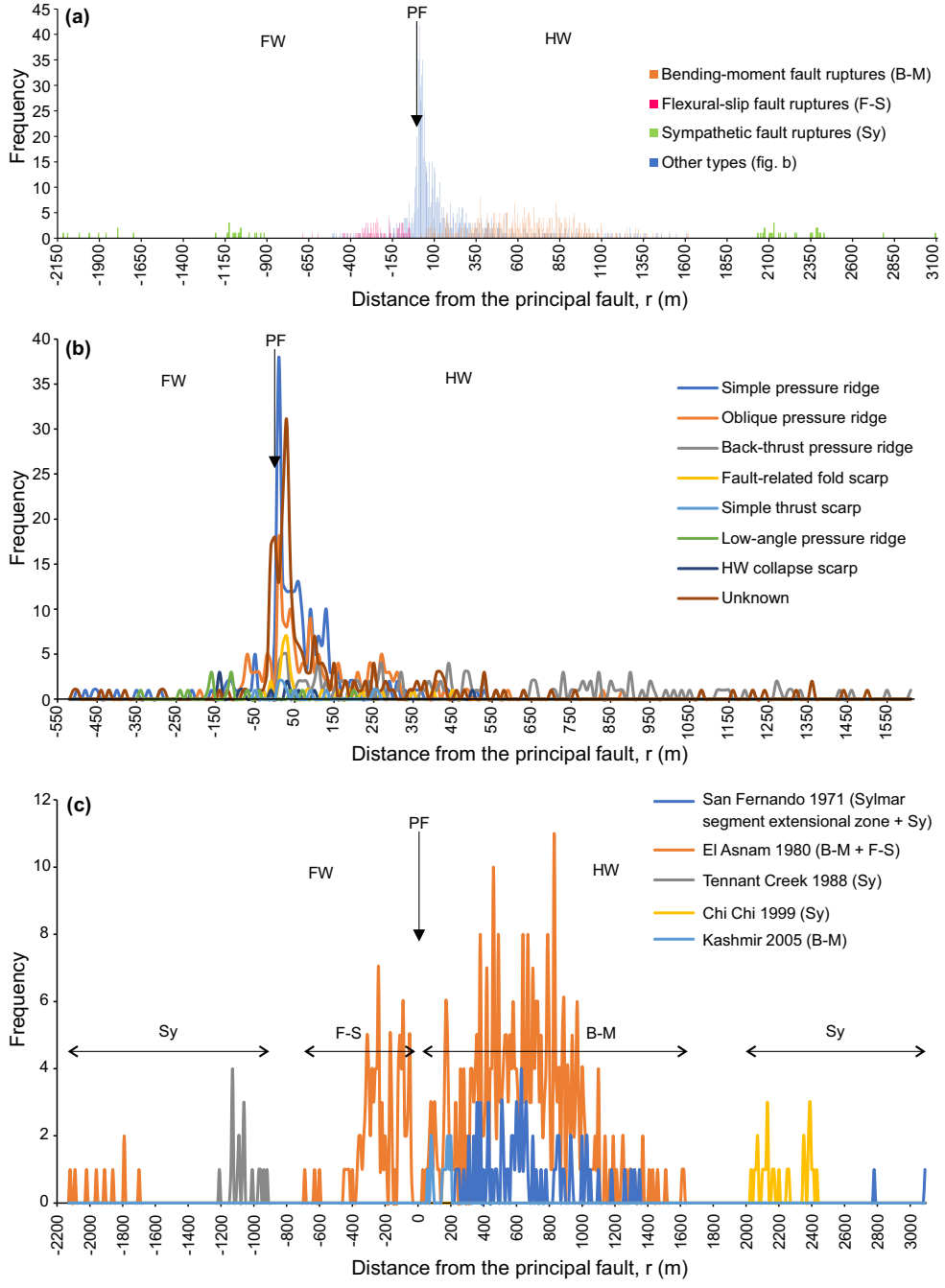

Figure 3. **(a)** Frequency distribution histogram of distributed rupture distance (r) from the PF rupture (PF) for all the earthquakes reported in Table 1. The positive and negative values refer to the data on the hanging wall and the footwall, respectively. **(b)** Frequency distribution curves of each scarp type excluding those associated with B-M, F-S and Sy fault ruptures (types h and i of Fig. 2 and sympathetic slip triggered on distant faults). **(c)** Frequency distribution curves of the B-M, F-S and Sy fault ruptures distinguished by earthquakes (the Sylmar segment extensional zone of the San Fernando 1971 earthquake rupture is included in the B-M fault ruptures).

The footwall data (Fig. 4c and d) has a modal value of the best fitting probability density function of 5 m. By applying the same percentiles used for the hanging wall, a 90 % cut off (FW90) was found at a distance of ~ 265 m from the PF. The FW75, FW50 and FW35 correspond to distances of ~ 120, ~ 45 and ~ 20 m from the PF, respectively (Table 2a). It is worth noticing that also for the footwall the 35 % probability corresponds to a sharp drop of the data.

Using the values calculated above, the ratio between the WRZ on the footwall and the WRZ on the hanging wall

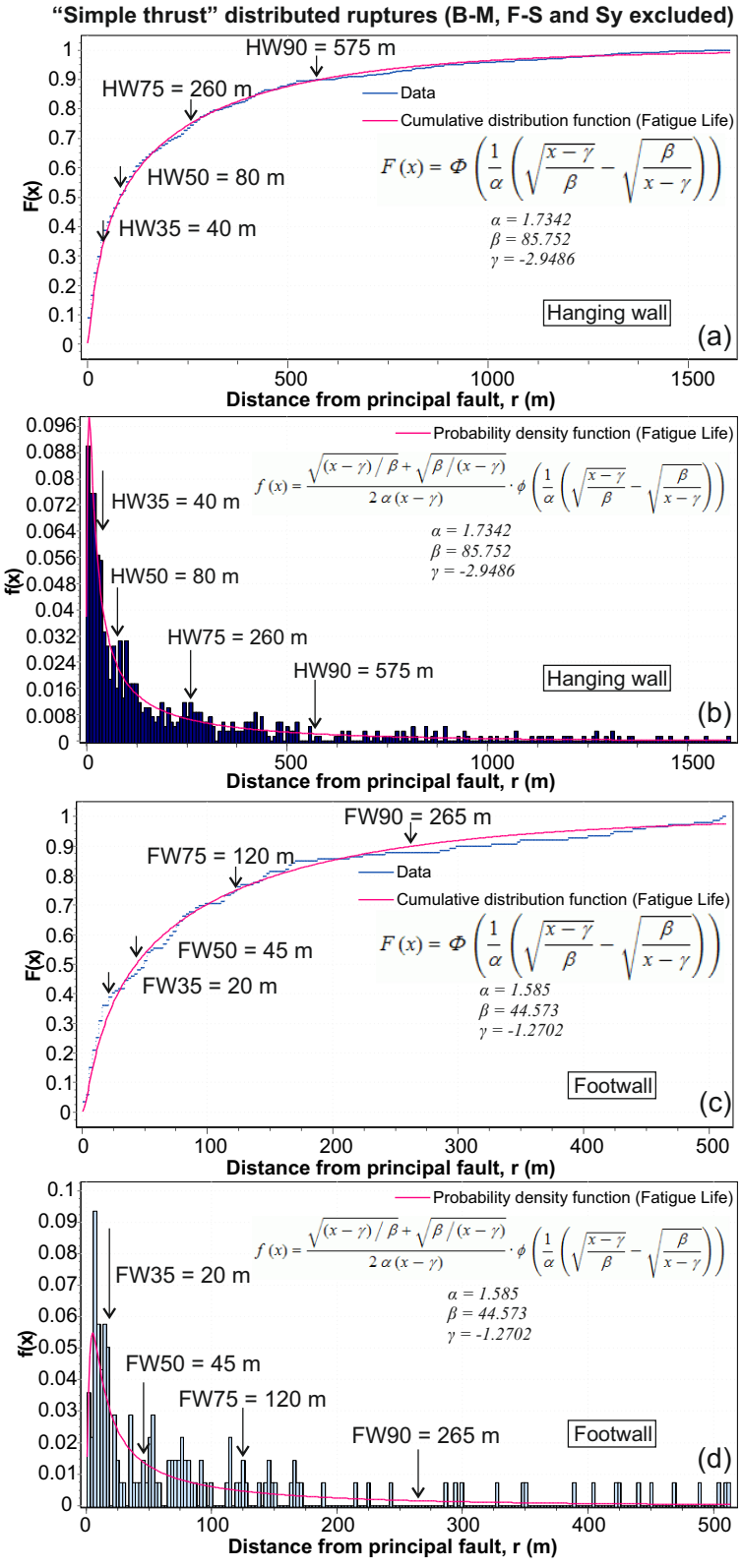

Figure 4. Cumulative distribution function and probability density function of the rupture distance (r) from the PF for the hanging wall (**a, b**, respectively) and the footwall (**c, d**, respectively) of the PF. Only the scarp types without associated B-M, F-S or sympathetic fault ruptures ("simple thrust" DRs) were analysed. The 35 % probability (HW35) is indicated because it corresponds to a sharp drop of the data in the histograms.

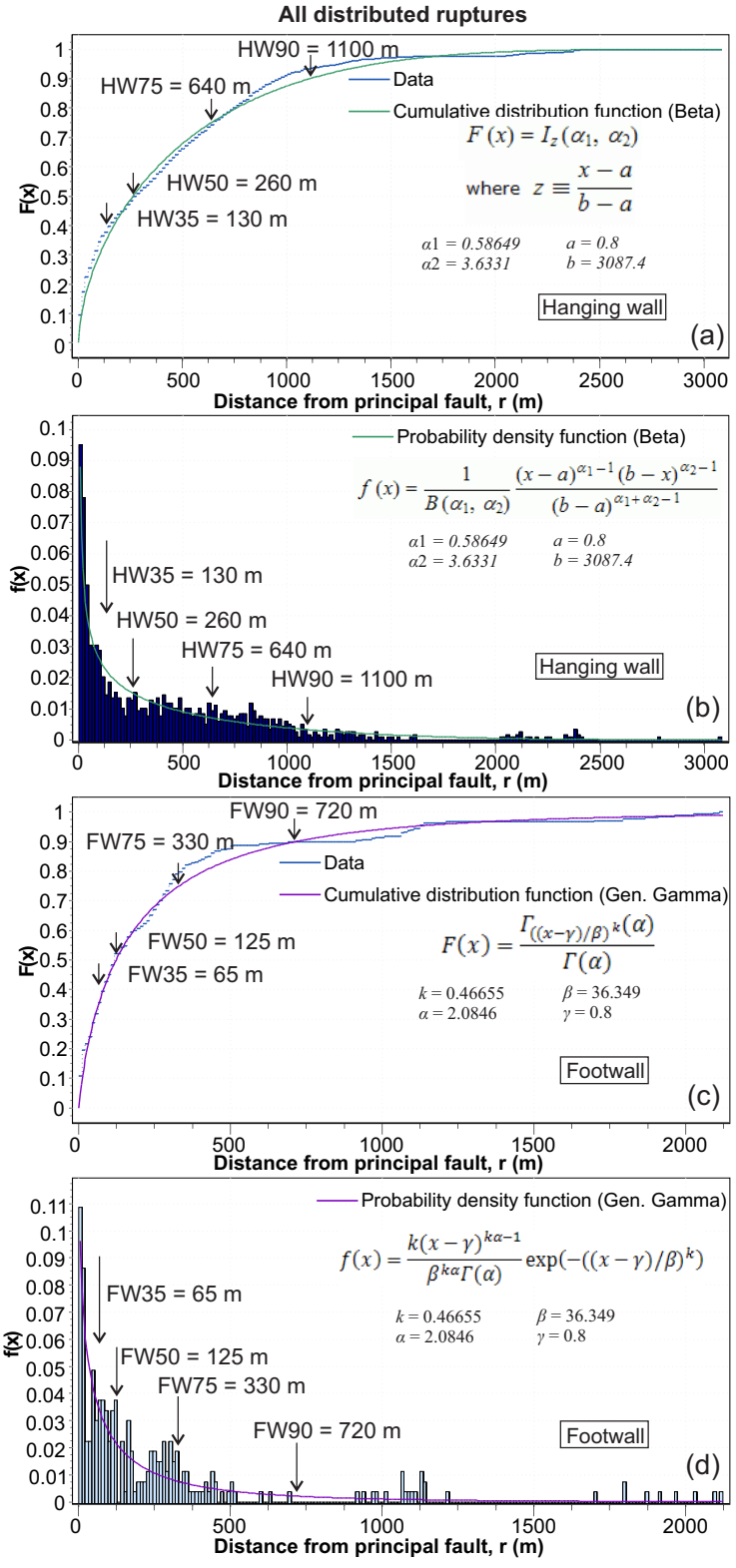

Figure 5. Cumulative distribution function and probability density function of the rupture distance (r) from the PF for the hanging wall (**a, b**, respectively) and the footwall (**c, d**, respectively) of the PF. All types of DRs were considered. The 35 % probability (HW35) is indicated for comparison with "simple thrust" database (Fig. 4), but it does not correspond to particular drops of the data in the histograms.

Table 2. Width of the rupture zone (WRZ) on the hanging wall (HW) and on the footwall (FW) and FW to HW ratio for **(a)** "simple thrust" DRs (B-M, F-S and Sy excluded) and **(b)** all DRs.

(a)	Probability[a]	WRZ HW	WRZ FW	Total WRZ	FW : HW
	90 %	575 m	265 m	840 m	1 : 2.2
	75 %	260 m	120 m	380 m	1 : 2.2
	50 %	80 m	45 m	125 m	1 : 1.8
	35 %[b]	40 m	20 m	60 m	1 : 2
(b)	Probability[a]	WRZ HW	WRZ FW	Total WRZ	FW : HW
	90 %	1100 m	720 m	1820 m	1 : 1.5
	75 %	640 m	330 m	970 m	1 : 1.9
	50 %	260 m	125 m	385 m	1 : 2.1
	35 %[c]	130 m	65 m	195 m	1 : 2

[a] Probabilities refer to the cumulative distribution functions of Figs. 4 (Table a) and 5 (Table b).
[b] Corresponding to a sharp drop of data in the histograms of Fig. 4, close to the PF.
[c] Calculated for comparison with "simple thrust" database, but not corresponding to particular drops of data in the histograms of Fig. 5.

ranges from 1 : 1.8 to 1 : 2.2 (Table 2a). Therefore, it is always close to 1 : 2 independently of the percentile used.

The results of the analysis performed on the entire database of distributed ruptures, including also the more complex B-M, F-S and Sy fault ruptures, is illustrated in Fig. 5 and summarized in Table 2b. As expected, the WRZ is significantly larger than for "simple thrust" DRs. The HW90, HW75 and HW50 correspond to distances of $\sim$ 1100, $\sim$ 640 and $\sim$ 260 m from the PF, respectively. For comparison with the "simple thrust" DRs, also the HW35 was calculated ($\sim$ 130 m), but it does not correspond with a particular drop of the data in the histogram of Fig. 5b. Instead, a sharp drop is still visible at a distance of $\sim$ 40 m from the PF. In the footwall, the FW90, FW75 and FW50 correspond to distances of $\sim$ 720 m, $\sim$ 330 m and $\sim$ 125 m from the PF, respectively. The FW35 corresponds to a distance of $\sim$ 65 m, but the sharp drop of the data in the histogram of Fig. 5d is at a distance of $\sim$ 20 m from the PF, as for the "simple thrust" database.

In order to analyse the potential relationships between WRZ and the earthquake size, in Fig. 6 the total WRZ (WRZ tot = WRZ hanging wall + WRZ footwall) is plotted against M_w (Fig. 6a) and, for the subset of data having displacement information, against the vertical displacement (VD) on the PF (Fig. 6b). The vertical displacement measured at the ground surface is highly sensitive to the shallow geometry of the thrust plane. The net displacement along the slip vector is a more appropriate parameter for considering the size of the displacement at the surface. However, the net displacement is rarely given in the literature, or can be obtained only by assuming a fault dip, while VD is the most commonly measured parameter. Therefore, we used VD as a proxy of the amount of surface displacement. In Fig. 6a a positive relation between the total WRZ and M_w is clear, particularly if sympathetic (Sy) fault ruptures are not considered. In fact, Sy data appear detached from the other data, suggesting that their occurrence is only partially dependent on the magnitude of the mainshock. They also depend on the structural features of the area, such as (1) whether or not an active, favourably oriented fault is present, and (2) its distance from the main seismogenic source. A correlation between the total WRZ and VD is not obvious (Fig. 6b). Even for small values of VD (< 1 m) the total WRZ can be as wide as hundreds of metres, but a larger number of displacement data are necessary for drawing convincing conclusions.

4 Comparison with Italian guidelines and implications for fault zoning during seismic microzonation

The definition of the WRZ based on the analysis of the data from worldwide thrust earthquakes can support the evaluation and mitigation of SFRH. The values reported in Table 2 can be used for shaping and sizing fault zones (e.g. warning or susceptible zones in the Italian guidelines; earthquake fault zones in the A-P Act) and avoidance zones around the trace of active thrust faults (Table 3).

The first question that needs to be answered is which set of data between "simple thrust" DRs (Fig. 4; Table 2a) and all DRs (Fig. 5, Table 2b) is the most appropriate to be used for sizing the fault zones. The answer is not easy and implicates some subjective choices. In Table 3 we suggest using the results from "simple thrust" DRs. The results from all DRs can be used in areas with poor geologic knowledge, in order to assess the extent of the area within which potential sources of fault displacement hazard can be present. Our choices result from the following lines of reasoning:

(1) The data analysed in this work are from brittle rupture of the ground surface. The measured DRs are always associated with surface faulting on the PF. Therefore, the results can be used for zoning the hazard deriving from mechanisms connected with the propagation of the rupture on the main fault plane up to the

Table 3. Comparison between fault zone size from Italian guidelines and the WRZ from the present study (proposal for integrating fault zoning for thrust faults). PF: principal fault rupture; DR: distributed ruptures; SFRH: surface fault rupture hazard.

Zone[a]	Seismic microzonation[b]	Italian guidelines	Proposed widths of zones from total WRZ (from "simple thrust" DR[c])	FW : HW[e]	Total WRZ from all DR (including B-M, F-S and Sy)
Warning zone (Zona di attenzione, ZA)	Basic (Level 1)	400 m (FW : HW = 1 : 2)	∼ 400 m (380 m) if 75 % prob. is considered or 840 m if 90 % prob. is considered (more precautionary; all the reasonably inferred hazard from PF and DR)	1 : 2	1800 m
Avoidance zone (Zona di rispetto, ZR)	High level (Level 3)	30 m (FW : HW = 1:2)	60 m (35 % prob.[d], very high hazard)	1 : 2	(90 % prob., applicable in poorly known areas for assessing the total extent of all potential SFRH)
Susceptible zone (Zona di suscettibilità, ZS)	High level (Level 3)	160 m (FW : HW = 1 : 2)	Variable (depending on the detail of Level 3 MS and structural complexity) Could be 380 m in the absence of particular constraints (75 % prob.; precautionary)	1 : 2	

[a] The original names of zones in the Italian guidelines (in Italian) are in italics.
[b] For different levels of seismic microzonation, refer to SM Working Group (2015).
[c] B-M, F-S and Sy fault ruptures are not included.
[d] Corresponding to a sharp drop of data in the histograms of Fig. 4.
[e] The computed values (Table 2) have been rounded to 1 : 2.

surface. Deformations associated with blind thrusting were not analysed. Therefore, the results are not suitable for zoning ductile tectonic deformations associated with blind thrusting (e.g. folding). Clearly, coseismic folding occurs both during blind thrusting and surface faulting thrusting. Furthermore, brittle surface ruptures and other ductile deformations can be strictly connected to each other, making it difficult to separate the two components, but a global analysis of the entire spectrum of permanent tectonic deformation associated with thrust faulting need additional data not considered here.

(2) In most cases, DRs occur on secondary structures that are small and cannot be recognized before the earthquake, or that only site-specific investigations could distinguish. Fault zones should include the hazard from this kind of ruptures.

(3) Some secondary faults connected with the PF can be sufficiently large to have their own geologic and geomorphic signature, and can be recognized before the earthquake. Most likely, close to the surface these structures behave similarly to the PF, with their own DRs. Faults with these characteristics should have their own zone, unless they are included in the PF zone.

(4) Point 3 also applies to distant large active faults that can undergo sympathetic triggering. They should be zoned as separate PFs. Using Sy fault ruptures for shaping zones of fault rupture hazard would imply distributing the hazard within areas that can be very large (Figs. 5 and 6). The size of the resulting zone would depend mostly on the structural setting of the analysed areas (presence or not of the fault, distance from the seismogenic source) rather than the mechanics which controls distributed faulting in response to principal faulting.

(5) B-M and F-S fault ruptures are not always present. Where present, they occur over distances ranging from hundreds of metres to kilometres (Fig. 3c). In any case, B-M and F-S secondary faults are strictly related to the structural setting of the area (large-scale folding; fold shape, wavelength and tightness; stiffness of folded strata). In fact, B-M fault ruptures commonly observed in historical earthquakes are normal faults. B-M normal faults are expected to occur in the shallowest convex (lengthened) layer of the folded anticline. They

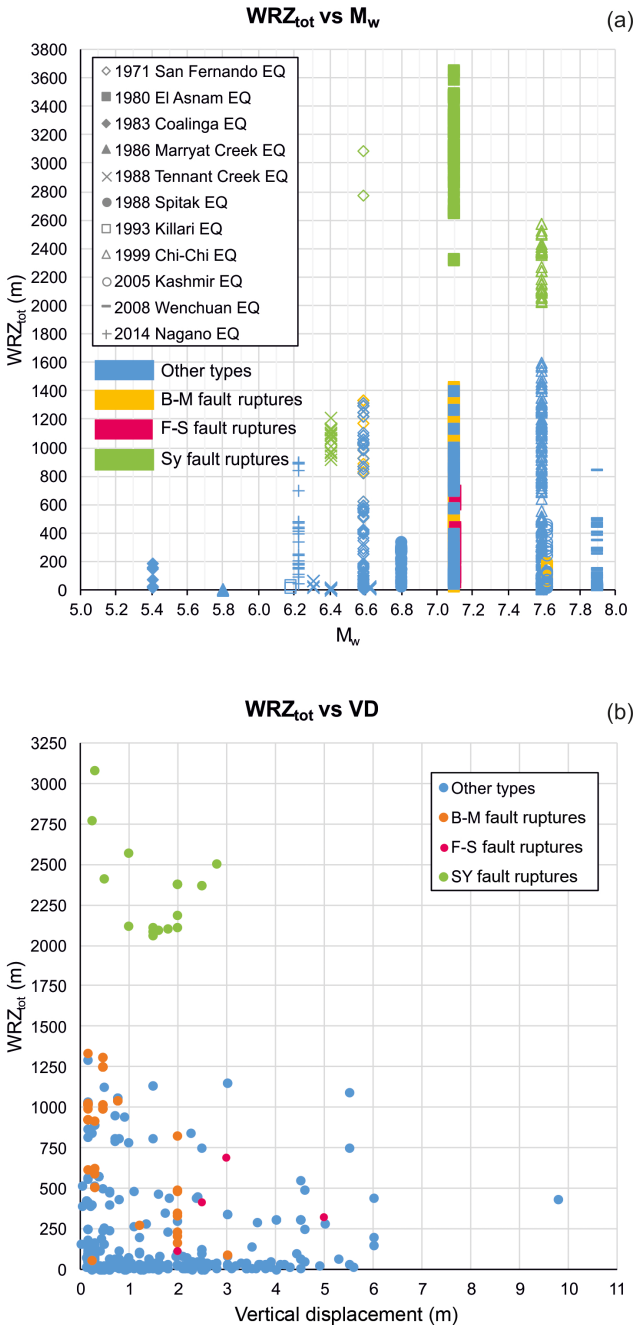

Figure 6. **(a)** Diagram plotting the total WRZ (WRZ_{tot} = WRZ hanging wall + WRZ footwall) against **(a)** the earthquake magnitude (M_w) and **(b)** the vertical displacement (VD) on the PF.

can occur only where the bending stress is tensional, that is the convex side of the folded layer, preferentially close to the crest of the anticline and parallel to the anticline hinge. F-S faults can rupture the surface where the steeply dipping limb of a fold is formed by strata of stiff rocks able to slip along bedding planes (e.g. Fig. 2i). Moreover, it is known that coseismic B-M or F-S faults often reactivate pre-existing fault scarps (e.g. Yeats, 1986), which might help in zoning the associated potential fault rupture hazard before the earthquake. Therefore, knowledge of the structural setting of the area can help in identifying zones potentially susceptible to B-M or F-S faulting, which should be zoned as separate sources of fault rupture hazard.

In Table 3, the total WRZ from the present study is compared with the sizes of the zones proposed by the Italian guidelines for SM studies (Technical Commission for Seismic Microzonation, 2015; SM Working Group, 2015). The total WRZ from "simple thrust" DRs is suggested to be used for sizing warning zones (Level 1 SM) and susceptible and avoidance zones (Level 3 SM).

The total WRZ from all DRs is suggested to be used for assessing the total extent of all potential surface fault rupture hazard in areas with poor geologic knowledge. This can have applications in selecting the area for investigation in studies for siting and designing critical and spatially distributed (e.g. pipelines) facilities.

The first observation is that the FW : HW ratio proposed by the Italian guidelines is supported by the results of this study (FW : HW ratio close to 1 : 2).

Assuming that the 90 % probability is a reasonable criterion for cutting the outliers from the analysed population, the resulting total WRZ (HW + FW) for "simple thrust" DRs is 840 m (560 m on the HW + 280 m on the FW). This width could be used for zoning all the reasonably inferred fault rupture hazard, from both the PF and DRs, during basic (Level 1) SM studies, which do not require high-level specific investigations. The obtained value is significantly different from that recommended by the Italian guidelines for Level 1 SM (400 m). The width of the zone remains close to ∼ 400 m (380 m) only if it is assumed that the 75 % probability (3 out of 4 probability that secondary faulting lies within the zone) is a sufficiently precautionary choice.

Another significant difference between our proposal and the Italian guidelines concerns also the width of the zone that should be avoided, due to the very high likelihood of having surface ruptures. Though the entire rupture zone could be hundreds of metres wide, more than one-third of DRs are expected to occur within a narrow, 60 m wide zone. As it could be expected, only site-specific palaeoseismologic investigations can quantify the hazard from surface faulting at a specific site. In the absence of such a detail, and when regarding larger areas (e.g. municipality scale) the fault avoidance zone should be of the order of 60 m, shaped asymmetrically compared to the trace of the main fault (40 m on the HW; 20 m on the FW).

In Table 3 a width of 380 m is proposed for the susceptible zone (Level 3 SM). The choice of defining the width of the zone as the third quartile is rather arbitrary. In fact, the width of the susceptible zone should be flexible. Susceptible zones are used only if uncertainties remain also after high-

level seismic microzonation studies, such as uncertainties on the location of the main fault trace or about the possibility of secondary faulting away from the main fault. Susceptible zones can also be used for areas where a not better quantifiable distributed faulting might occur, such as in structurally complex zones (e.g. stepovers between main fault strands).

5 Conclusions

The distribution of coseismic surface ruptures (distance of DRs from the PF rupture) for 11 well-documented historical surface faulting thrust earthquakes ($5.4 \leq M \leq 7.9$) provide constraints on the general characteristics of the surface rupture zone, with implications for zoning the surface rupture hazard along active thrust faults.

Distributed ruptures can occur up to large distances from the PF (up to ~ 3000 m on the hanging wall), but most of them occur within few dozens of metres from the PF. The distribution of secondary ruptures is asymmetric, with most of them located on the hanging wall. Coseismic folding of large-scale folds (hundreds of metres to kilometres in wavelength) may produce bending-moment (B-M) or flexural-slip (F-S) fault ruptures, widening significantly the rupture zone. Additional widening of the rupture zone can be due to sympathetic slip on distant active faults (Sy fault ruptures).

The distribution of secondary ruptures for "simple thrust" ruptures (without B-M, F-S, and Sy fault ruptures) can be fitted by a continuous probability density function, of the same form for both the hanging wall and footwall. This function can be used for removing outliers from the analysed database (e.g. 90 % probability) and define criteria for shaping SFRH zones. These zones can be used during seismic microzonation studies and can help in integrating existing guidelines. More than one-third of the ruptures are expected to occur within a zone of ~ 60 m wide. This narrow zone could be used for defining the fault-avoiding zone during high-level, municipality-scale seismic microzonation studies (i.e. Level 3 SM according to the Italian guidelines). The average FW : HW ratio of the WRZ is close to 1 : 2, independently of the percentile used.

In addition to the expected rupture zone along the trace of the main thrust, zones potentially susceptible to B-M or F-S secondary faulting can be identified by detailed structural study of the area (shape, wavelength, tightness and lithology of the thrust-related large-scale folds) and by scrutinizing possible geomorphic traces of past secondary faulting. Where recognized, these areas should have their own zones of fault rupture hazard.

The analysis of the entire database of DRs (Fig. 5) indicates significantly larger rupture zones compared to the database without B-M, F-S and Sy fault ruptures ("simple thrust" DRs). This is due to the combination of processes related to the propagation up to the surface of the main fault rupture and other processes associated with large-scale coseismic folding, as well as triggering of distant faults. The results from the entire database of DRs can be useful in poorly known areas, in order to assess the extent of the area within which potential sources of fault displacement hazard can be present.

The results of this study can be used for improving the attenuation relationships for distributed faulting with distance from the principal fault, with possible applications in probabilistic studies of fault displacement hazard (e.g. Youngs et al., 2003; Petersen et al., 2011).

Data availability. The database of DRs used for the statistical analysis of WRZ (Table S1) and the figures illustrating the measurements carried out on published maps (Figs. S1 to S11) are provided in the Supplement of this paper.

The Supplement related to this article is available online at https://doi.org/10.5194/nhess-18-241-2018-supplement.

Special issue statement. This article is part of the special issue "Linking faults to seismic hazard assessment in Europe". It is not associated with a conference.

Competing interests. The authors declare that they have no conflict of interest.

Acknowledgements. The project was funded by DiSPuTer (Department of Psychological, Health and Territorial Sciences), "G. D'Annunzio" University of Chieti-Pescara (research funds to Paolo Boncio).

Edited by: Francesco Visini
Reviewed by: Franz Livio and one anonymous referee

References

Angelier, J., Lee, J. C., Chu, H. T., and Hu, J. C.: Reconstruction of fault slip of the September 21st, 1999, Taiwan earthquake in the asphalted surface of a car park, and co-seismic slip partitioning, J. Struct. Geol., 25, 345–350, 2003.

Avouac, J. P., Ayoub, F., Leprince, S., Konea, O., and Helmberger, V.: The 2006 M_w 7.6 Kashmir earthquake: sub-pixel correlation of ASTER images and seismic waveforms analysis, Earth Planet. Sc. Lett., 249, 514–528, 2006.

Bilham, R. and Yu, T. T.: The morphology of thrust faulting in the 21 September 1999, Chichi, Taiwan earthquake, J. Asian Earth Sci., 18, 351–367, 2000.

Boncio, P., Galli, P., Naso, G., and Pizzi, A.: Zoning surface rupture hazard along normal faults: insight from the 2009 M_w 6.3 L'Aquila, Central Italy, earthquake and other

global earthquakes, B. Seismol. Soc. Am., 102, 918–935, https://doi.org/10.1785/0120100301, 2012.

Bowman, J. R. and Barlow, B. C.: Surveys of the Fault Scarp of the 1986 Marryat Creek, South Australia, Earthquake, [Australian] Bureau of Mineral Resources, Geology and Geophysics, Canberra, AU, BMR Record 1991/190, 12 pp., 3 plates, 1991.

Bryant, W. A. and Hart, E. W.: Fault-Rupture Hazard Zones in California, Alquist-Priolo Earthquake Fault Zoning Act With Index to Earthquake Fault Zones Maps, Calif. Geol. Surv., Sacramento, CA, Spec. Pub. 42, Interim Revision 2007, 41 pp., 2007.

Central Geological Survey, MOEA at http://gis.moeacgs.gov.tw/gwh/gsb97-1/sys8/index.cfm, last access: October 2017.

Chang, J. C. and Yang, G. S.: Deformation and occurrence of the Che-lung-pu Fault from geomorphic evidence, Quatern. Int., 115–116, 177–188, 2004.

Chen, C. H., Chou, H. S., Yang, C. Y., Shieh, B. J., and Kao, Y. H.: Chelungpu fault inflicted damages of pile foundations on FWY rout 3 and Fault zoning regulations in Taiwan, in: Proceedings of the JSCE/EqTAP Workshop on Seismic Fault-induced Failures, Tokyo, Japan, 22 February 2003, 1–19, 2003.

Chen, G. H., Xu, X. W., Zheng, R. Z., Yu, G. H., Li, F., Li, C. X., Wen, X. Z., He, Y. L., Ye, Y. Q., Chen, X. C., and Wang, Z. C.: Quantitative analysis of the co-seismic surface rupture of the 2008 Wenchuan earthquake, Sichuan, China along the Beichuan-Yingxiu Fault, Seismol. Geol., 30, 723–738, 2008 (in Chinese with English abstract).

Chen, W. C., Chu, H. T., and Lai, T. C.: Surface ruptures of the Chi-Chi Earthquake in the Shihgang Dam area, Special Issue for the Chi-Chi Earthquake, 1999, Central Geological Survey, MOEA, Taipei, Taiwan, Spec. Pub. 12, 41–62, 2000 (in Chinese with English abstract).

Crone, A. J., Machette, M. N., and Bowman, J. R.: Geologic investigations of the 1988 Tennant Creek, Australia, earthquakes – implications for paleoseismicity in stable continental regions, US Geol. Surv., Denver, CO, Bull. 2032-A, 51 pp., 2 plates, 1992.

Dong S, Zhang Y, Wu Z, Yang, N., Ma, Y., Shi, W., Chen, Z., Long, C., and An, M.: Surface rupture and co-seismic displacement produced by the M_S 8.0 Wenchuan earthquake of May 12th, 2008, Sichuan, China: eastwards growth of the Qinghai-Tibet Plateau, Acta Geol. Sin.-Engl., 82, 938–948, 2008a.

Dong, S., Han, Z., and An, Y.: Surface deformation at the epicenter of the May 12, 2008 Wenchuan M8 Earthquake, at Yingxiu Town of Sichuan Province, China, Sci. China Ser. E, 51, 154–163, https://doi.org/10.1007/s11431-008-6007-0, 2008b.

Faccioli, E., Anastasopoulos, I., Gazetas, G., Callerio, A., and Paolucci, R.: Fault rupture–foundation interaction: selected case histories, B. Earthq. Eng., 6, 557–583, 2008.

Fredrich, J., McCaffrey, R., and Denham, D.: Source parameters of seven large Australian earthquakes determined by body waveform inversion, Geophys. J.+, 95, 1–13, 1988.

Haessler, H., Deschamps, A., Dufumier, H., Fuenzalida, H., and Cisternas, A.: The rupture process of the Armenian earthquake from broad-band teleseismic body wave records, Geophys. J. Int., 109, 151–161, 1992.

Huang, C., Chan, Y. C., Hu, J. C., Angelier, J., and Lee, J. C.: Detailed surface co-seismic displacement of the 1999 Chi-Chi earthquake in western Taiwan and implication of fault geometry in the shallow subsurface, J. Struct. Geol., 30, 1167–1176, 2008.

Huang, W. J.: Deformation at the Leading Edge of Thrust Faults, PhD dissertation, Purdue University, West Lafayette, Indiana, 435 pp., 2006.

Huang, W. J., Chen, Z. Y., Liu, S. Y., Lin, Y. H., Lin, C. W., and Chang, H. C.: Surface deformation models of the 1999 Chi–Chi earthquake between Tachiachi and Toupienkengchi, central Taiwan, Special Issue for the Chi-Chi Earthquake, 1999, Central Geological Survey, MOEA, Taipei, Taiwan, Spec. Pub. 12, 63–87, 2000 (in Chinese with English abstract).

Ishimura, D., Okada, S., Niwa, Y., and Toda, S.: The surface rupture of the 22 November 2014 Nagano-ken-hokubu earthquake (M_W 6.2), along the Kamishiro fault, Japan, Active Fault Research, 43, 95–108, 2015 (in Japanese with English abstract).

Kaneda, H., Nakata, T., Tsutsumi, H., Kondo, H., Sugito, N., Awata, Y., Akhtar, S. S., Majid, A., Khattak, W., Awan, A. A., Yeats, R. S., Hussain, A., Ashraf, M., Wesnousky, S. G., and Kausar, A. B.: Surface rupture of the 2005 Kashmir, Pakistan, Earthquake and its active tectonic implications, B. Seismol. Soc. Am., 98, 521–557, 2008.

Kawashima, K.: Damage of bridges resulting from fault rupture in the 1999 Kocaeli and Dunce, Turkey earthquakes and the 1999 Chi-Chi, Taiwan earthquake, Structural Eng./Earthquake Eng., JSCE, 19, 179s–197s, 2002.

Kelson, K. I., Kang, K. H., Page, W. D., Lee, C. T., and Cluff, L. S., 2001: Representative styles of deformation along the Chelungpu Fault from the 1999 Chi-Chi (Taiwan) earthquake: geomorphic characteristic and responses of man-made structures, B. Seismol. Soc. Am., 91, 930–952, 2001.

Kelson, K. I., Koehler, R. D., Kang, K.-H., Bray, J. D., and Cluff, L. S.: Surface deformation produced by the 1999 Chi-chi (Taiwan) earthquake and interactions with built structures, William Lettis & Associates, Inc., Walnut Creek, CA, Final Technical Report submitted to US Geol. Surv., Award No. 01-HQ-GR-0122,, 21 pp., 2003.

Kerr, J., Nathan, S., Van Dissen, R., Webb, P., Brunsdon, D., and King, A.: Planning for development of land on or close to active faults: a guide to assist resource management planners in New Zealand, Report prepared for the Ministry for the Environment by the Institute of Geological & Nuclear Sciences, Client Report 2002/124, Project Number 440W3301, Wellington, NZ, 2003.

Konagai, K., Hori, M., Meguro, K., Koseki, J., Matsushima, T., Johansson, J., and Murata, O.: Key Points for Rational Design for Civil Infrastructures near Seismic Faults Reflecting Soil-Structure Interaction Features, Japan Geotechnical Society, Tokyo, JP, Report of JSPS research project, grant-in-aid for scientific research (A) Project No. 16208048, 146 pp., 2006.

Kumahara, Y. and Nakata, T.: Recognition of active faults generating the 2005 Pakistan earthquake based on interpretation of the CORONA satellite photographs, E-journal GEO, 2, 72–85, 2007 (in Japanese with English abstract).

Lee, G. C. and Loh, C. H. (Eds): The Chi-Chi, Taiwan Earthquake of September 21, 1999: Reconnaissance Report, Multidisciplinary Center for Earthquake Eng. Res., Buffalo, NY, Technical Report MCEER-00-0003, 144 pp., 2000.

Lee, J. C. and Chan, Y. C.: Structure of the 1999 Chi-Chi earthquake rupture and interaction of thrust faults in the active fold belt of western Taiwan, J. Asian Earth Sci., 31, 226–239, 2007.

Lee, J. C., Chen, Y. G., Sieh, K., Mueller, K., Chen, W. S., Chu, H. T., Chan, Y. C., Rubin, C., and Yeats, R.: A vertical

exposure of the 1999 surface rupture of the Chelungpu Fault at Wufeng, Western Taiwan: structural and paleoseismic implications for an active thrust fault, B. Seismol. Soc. Am., 91, 5, 914–929, 2001.

Lee, Y. H., Hsieh, M. L., Lu, S. D., Shih, T. S., Wu, W. Y., Sugiyama, Y., Azuma, T., and Kariya, Y.: Slip vectors of the surface rupture of the 1999 Chi-Chi earthquake, western Taiwan, J. Struct. Geol., 25, 1917–1931, 2003.

Lee, Y. H., Wu, K. C., Rau, R. J., Chen, H. C., Lo, W., and Cheng, K. C.: Revealing coseismic displacements and the deformation zones of the 1999 Chi-Chi earthquake in the Tsaotung area, central Taiwan, using digital cadastral data, J. Geophys. Res., 115, B03419, https://doi.org/10.1029/2009JB006397, 2010.

Lettis, W. R., Wells, D. L., and Baldwin, J. N.: Empirical observations regarding reverse earthquakes, blind thrust faults, and quaternary deformation: are blind thrust faults truly blind?, B. Seismol. Soc. Am., 87, 1171–1198, 1997.

Lin, A., Sano, M., Yan, B., and Wang, M.: Co-seismic surface ruptures produced by the 2014 M_w 6.2 Nagano earthquake, along the Itoigawa–Shizuoka tectonic line, central Japan, Tectonophysics, 656, 142–153, 2015.

Lin, W. H.: On surface deformations from the Chi-Chi earthquake in the Shihkang and Chutzekeng areas, Special Issue for the Chi-Chi Earthquake, 1999, Central Geological Survey, MOEA, Taipei, Taiwan, Spec. Pub. 12, 1–17, 2000 (in Chinese with English abstract).

Liu-Zeng, J., Zhang, Z., Wen, L., Tapponnier, P., Sun, J., Xing, X., Hu, G., Xu, Q., Zeng, L., Ding, L., Ji, C., Hudnut, K. W., and van der Woerd, J.: Co-seismic ruptures of the 12 May 2008, M_s 8.0 Wenchuan earthquake, Sichuan: east–west crustal shortening on oblique, parallel thrusts along the eastern edge of Tibet, Earth Planet. Sc. Lett., 286, 355–370, 2009.

Liu-Zeng, J., Sun, J., Zhang, Z., Wen, L., Xing, X., Hu, G., and Xu, Q.: Detailed mapping of surface rupture of the Wenchuan Ms 8.0 earthquake near Hongkou and seismotectonic implications, Quaternary Sciences, 30, 1–29, 2010 (in Chinese with English abstract).

Liu-Zeng, J., Sun, J., Wang, P., Hudnut, K. W., Ji, C., Zhang, Z., Xu, Q., and Wen, L.: Surface ruptures on the transverse Xiaoyudong fault: a significant segment boundary breached during the 2008 Wenchuan earthquake, China, Tectonophysics, 580, 218–241, 2012.

Machette, M. N., Crone, A. J., and Bowman, J. R.: Geologic investigations of the 1986 Marryat Creek, Australia, earthquakes – implications for paleoseismicity in stable continental regions, US Geol. Surv., Denver, CO, Bull. 2032-B, 29 pp., 2 plates, 1993.

McCaffrey, R.: Teleseismic investigation of the January 22, 1988 Tennant Creek, Australia, earthquakes, Geophys. Res. Lett., 16, 413–416, 1989.

Meghraoui, M., Jaegy, R., Lammali, K., and Albarède, F.: Late Holocene earthquake sequences on the El Asnam (Algeria) thrust fault, Earth Planet. Sc. Lett., 90, 187–203, 1988.

Okada, S., Ishimura, D., Niwa, Y., and Toda, S.: The first surface-rupturing earthquake in 20 years on a HERP active fault is not characteristic: the 2014 M_w 6.2 Nagano event along the northern Itoigawa–Shizuoka tectonic line, Seismol. Res. Lett., 86, 1–14, 2015.

Ota, Y., Huang, C. Y., Yuan, P. B., Sugiyama, Y., Lee, Y. H., Watanabe, M., Sawa, H., Yanagida, M., Sasaki, S., Suzuki, Y., Tang, H. S., Shu, U. T., Yang, S. Y., Hirouchi, D., and Taniguchi, K.: Trenching study at the Tsautun Site on the central part of the Chelungpu Fault, Taiwan, J. Geogr., 110, 698–707, 2001 (in Japanese with English abstract).

Ota, Y., Watanabe, M., Suzuki, Y., Yanagida, M., Miyawaki, A., and Sawa, H.: Style of the surface deformation by the 1999 Chichi earthquake at the central segment of Chelungpu fault, Taiwan, with special reference to the presence of the main and subsidiary faults and their progressive deformation in the Tsauton area, J. Asian Earth Sci., 31, 214–225, 2007a.

Ota, Y., Shishikura, M., Ichikawa, K., Watanabe, M., Yanagida, M., Tanaka, T., Sawa, H., Yamaguchi, M., Lee, Y. H., Lu, S. T., Shih, T. S., and Amagasa, S.: Low-angle reverse faulting during two earthquakes on the northern part of the Chelungpu fault, deduced from the Fengyuan trench, Central Taiwan, Terr. Atmos. Ocean. Sci., 18, 55–66, 2007b.

Petersen, M., Dawson, T. E., Chen, R., Cao, T., Wills, C. J., Schwartz, D. P., and Frankel, A. D.: Fault displacement hazard for strike-slip faults, B. Seismol. Soc. Am., 101, 805–825, 2011.

Philip, H. and Meghraoui, M.: Structural analysis and interpretation of the surface deformation of the El Asnam earthquake of October 10, 1980, Tectonics, 2, 17–49, 1983.

Philip, H., Rogozhin, E., Cisternas, A., Bousquet, J. C., Borisov, B., and Karakhanian, A.: The Armenian earthquake of 1988 December 7: faulting and folding, neotectonics and palaeoseismicity, Geophys. J. Int., 110, 141–158, 1992.

Rajendran, C. P., Rajendran, K., Unnikrishnan, K. R., and John, B.: Palaeoseismic indicators in the rupture zone of the 1993 Killari (Latur) earthquake, Curr. Sci. India, 70, 385–390, 1996.

Rymer, M. J., Kendrick, K. J., Lienkaemper, J. J., and Clark, M. M.: Surface rupture on the Nunez fault during the Coalinga earthquake sequence, in: The Coalinga, California, Earthquake of May 2, 1983, edited by: Rymer, M. J., Ellsworth, W. L., US Geol. Surv., Denver, CO, Prof. Paper 1487, 299–318, 1990.

Sayab, M. and Khan, M. A.: Temporal evolution of surface rupture deduced from coseismic multi-mode secondary fractures: insights from the October 8, 2005 (M_w 7.6) Kashmir earthquake, NW Himalaya, Tectonophysics, 493, 58–73, 2010.

Seeber, L., Ekstrom, G., Jain, S. K., Murty, C. V. R., Chandak, N., and Armbruster, J. G.: The 1993 Killari earthquake in central India: a new fault in Mesozoic basalt flows?, J. Geophys. Res.-Sol. Ea., 101, 8543–8560, https://doi.org/10.1029/95JB01865, 1996.

Shin, T. C. and Teng, T. L.: An overview of the 1999 Chi-Chi, Taiwan, Earthquake, B. Seismol. Soc. Am., 91, 895–913, 2001.

SM Working Group: Guidelines for Seismic Microzonation, Conference of Regions and Autonomous Provinces of Italy, Civil Protection Department, English edition of: Gruppo di lavoro MS, Indirizzi e criteri per la microzonazione sismica, Conferenza delle Regioni e delle Province autonome – Dipartimento della protezione civile, Roma, 2008, 3 vol. e Dvd, 2015, available at: http://www.protezionecivile.gov.it/httpdocs/cms/attach_extra/GuidelinesForSeismicMicrozonation.pdf (last access: October 2017), 2015.

Technical Commission for Seismic Microzonation: Linee guida per la gestione del territorio in aree interessate da Faglie Attive e Capaci (FAC), versione 1.0, Conferenza delle Regioni e

delle Province Autonome – Dipartimento della Protezione Civile, Rome, 55 pp., 2015 (in Italian).

Tsutsumi, H. and Yeats, R.: Tectonic setting of the 1971 Sylmar and 1994 Northridge earthquakes in the San Fernando valley, California, B. Seismol. Soc. Am., 89, 1232–1249, 1999.

US Geological Survey Staff: Surface faulting, in: The San Fernando, California, earthquake of February 9, 1971, US Geol. Surv., Washington, Prof. Paper 733, 55–76, 1971.

Wang, H., Ran, Y, Chen, L., Shi, X., Liu, R., and Gomez, F.:Determination of horizontal shortening and amount of reverse-faulting from trenching across the surface rupture of the 2008 M_w 7.9 Wenchuan earthquake, China, Tectonophysics, 491, 10–20, 2010.

Wells, D. and Coppersmith, K.: New empirical relationships among magnitude, rupture length, rupture width, rupture area, and surface displacement, B. Seismol. Soc. Am., 84, 974–1002, 1994.

Wesnousky, S. G.: Displacement and geometrical characteristics of earthquake surface ruptures: issues and implications for seismic hazard analysis and the earthquake rupture process, B. Seismol. Soc. Am., 98, 1609–1632, 2008.

Xu, X., Wen, X., Ye, J., Ma, B., Chen, J., Zhou, R., He, H., Tian, Q., He, Y., Wang, Z., Sun, Z., Feng, X., Yu, G., Chen, L., Chen, G., Yu, S., Ran, Y., Li, X., Li, C., and An, Y.: The Ms 8.0 Wenchuan earthquake surface ruptures and its seismogenic structure, Seismol. Geol., 30, 597–629, 2008 (in Chinese with English abstract).

Xu, X., Wen, X., Yu, G., Chen, G., Klinger, Y., Hubbard, J., and Shaw, J.: Co-seismic reverse- and oblique-slip surface faulting generated by the 2008 M_w 7.9 Wenchuan earthquake, China, Geology, 37, 515–518, https://doi.org/10.1130/G25462A.1, 2009.

Yeats, R. S.: Active faults related to folding, in: Active Tectonics: Impact on Society, The National Academies Press, Washington, 280 pp., https://doi.org/10.17226/624, 1986.

Yelding, G., Jackson, J. A., King, G. C. P., Sinvhal, H., Vita-Finzi, C., and Wood, R. M.: Relations between surface deformation, fault geometry, seismicity, and rupture characteristics during the El Asnam (Algeria) earthquake of the 10 October 1980, Earth Planet. Sc. Lett., 56, 287–304, 1981.

Youngs, R. R., Arabasz, W. J., Anderson, R. E., Ramelli, A. R., Ake, J. P., Slemmons, D. B., McCalpin, J. P., Doser, D. I., Fridrich, C. J., Swan III, F. H., Rogers, A. M., Yount, J. C., Anderson, L. W., Smith, K. D., Bruhn, R. L., Knuepfer, L. K., Smith, R. B., dePolo, C. M., O'Leary, D. W., Coppersmith, K. J., Pezzopane, S. K., Schwartz, D. P., Whitney, J. W., Olig, S. S., and Toro, G. R.: A methodology for probabilistic fault displacement hazard analysis (PFDHA), Earthq. Spectra, 19, 191–219, 2003.

Yu, G., Xu, X., Klinger, Y., Diao, G., Chen, G., Feng, X., Li, C., Zhu, A., Yuan, R., Guo, T., Sun, X., Tan, X., and An, Y.: Fault-Scarp Features and Cascading-Rupture Model for the M_w 7.9 Wenchuan Earthquake, Eastern Tibetan Plateau, China, B. Seismol. Soc. Am., 100, 2590–2614, 2010.

Yu, G. H., Xu, X. W., Chen, G. H., Gou, T. T., Tan, X. B., Yang, H., Gao, X., An, Y. F., and Yuan, R. M.: Relationship between the localization of surface ruptures and building damages associated with the Wenchuan 8.0 earthquake, Chinese J. Geophys., 52, 1294–1311, 2009.

Zhang, J. Y., Bo, J. S., Xu, G. D., and Huang, J. Y.: Buildings setbacks research from surface-fault-rupture statistical analysis, Appl. Mech. Mater., 204–208, 2410–2418, 2012.

Zhang, Y. S., Sun, P., Shi, J. S., Yao, X., and Xiong, T. Y.: Investigation of rupture influenced zones and their corresponding safe distances for reconstruction after 5.12 Wenchuan earthquake, Eng. Geol., 18, 312–319, 2010 (in Chinese with English abstract).

Zhang, Y. S., Shi, J. S., Sun, P., Yang, W., Yao, X., Zhang, C. S., and Xiong, T. Y.: Surface ruptures induced by the Wenchuan earthquake: their influence widths and safety distances for construction sites, Eng. Geol., 166, 245–254, 2013.

Zhou, Q., Xu, X., Yu, G., Chen, X., He, H., and Yin, G.: Width Distribution of the Surface Ruptures Associated with the Wenchuan Earthquake: implication for the Setback Zone of the Seismogenic Faults in Post-earthquake Reconstruction, B. Seismol. Soc. Am., 100, 2660–2668, 2010.